

Effects of pressure and temperature on the dielectric constant of GaS, GaSe, and InSe: Role of the electronic contribution

D. Errandonea,* A. Segura, and V. Muñoz

Instituto de Ciencia de Materiales, Departamento de Física Aplicada (Facultad de Física), Universidad de Valencia, C/Dr. Moliner 50, E-46100 Burjassot (Valencia), Spain

A. Chevy

Laboratoire de Physique des Milieux Condensés, Université Pierre et Marie Curie, 4 Place Jussieu, 75252 Paris, Cedex 05, France

(Received 13 July 1999)

In this work we report on direct measurements of the temperature and pressure dependences of the low-frequency dielectric constant along c axis (ϵ_{\parallel}) of GaS, GaSe, and InSe. The temperature dependence of both the ordinary and extraordinary refractive indexes is also presented. A large increase of ϵ_{\parallel} under pressure has been observed. In the framework of a rigid ion model, the lattice contribution to ϵ_{\parallel} is shown to increase slightly under pressure, due to the change of the angle between the anion-cation bond and the layer plane. Consequently, the pressure behavior of ϵ_{\parallel} is proposed to arise from a large increase of the electronic contribution to ϵ_{\parallel} . This fact is explained through a decrease of the Penn gap for polarization parallel to the c axis, whose energy and pressure coefficient are shown to scale with those of the indirect band gap in these compounds. A supplementary and reversible step increase of ϵ_{\parallel} is observed at 1.6 GPa in GaS, which is associated with a phase transition that has been already observed by other authors. [S0163-1829(99)11547-9]

I. INTRODUCTION

The pressure (P) and temperature (T) dependences of the dielectric constants of semiconductors are of current interest in semiconductors research. In principle, the study of these properties is an important issue because they enter in a non-trivial way into the underlying physics of transport, optical, and lattice-dynamical properties. Since the early work of Samara,¹ the effects of pressure and temperature on the low-frequency dielectric constant (ϵ) of tetrahedrally coordinated semiconductors are well known. In particular, the temperature dependence of ϵ has been shown to be controlled by anharmonicities in crystal potentials, yielding positive temperature coefficients.¹ Moreover, in the most representative semiconductors, it has been observed that ϵ decreases with increasing pressure, this phenomenon being a consequence of the reduction of both the electronic and lattice polarizabilities.¹

Nevertheless, in III-VI layered semiconductors a different behavior under pressure is expected. These semiconductors consist of two types of chemical bonding, depending on the crystallographic orientation. This strong crystal anisotropy affects both optical and transport properties.²⁻¹⁰ The application of pressure provides then a means to tune the degree of anisotropy in bonding. This leads to strong nonlinearities in the pressure dependence of physical properties.⁸⁻¹³ In particular, a large decrease of the excitonic binding energy has been observed in indium selenide⁹ (InSe) and gallium selenide¹⁰ (GaSe) under compression. It was attributed to the increase of the low-frequency dielectric constant parallel to the c axis (ϵ_{\parallel}). This behavior of ϵ_{\parallel} has been verified up to 1.2 GPa by direct measurements in gallium sulfide (GaS).¹⁴ Two models have been developed to explain it.¹⁰ One is the charge transfer hypothesis, which relates the variation of ϵ_{\parallel} to a charge transfer from intralayer to interlayer space. On

the other hand, the second model, which will be referred to as isotropy hypothesis, assumes that at about 5 GPa inter and intralayer forces become of the same order resulting in a nearly isotropic behavior of all physical parameters.

In this paper we study, by capacitance measurements, the pressure and temperature dependences of ϵ_{\parallel} in GaS, GaSe, and InSe. The maximum pressure was limited to 3 GPa. Furthermore, we have measured the temperature dependence of the refractive indexes of these materials. The experimental arrangements are briefly described in Sec. II and the following two sections are devoted to present and discuss the results. On the basis of these data and earlier results, we evaluate the influence of the lattice and electronic contributions on the behavior of ϵ_{\parallel} .

II. EXPERIMENTAL DETAILS

Single crystals of semi-insulating GaS and GaSe were grown by the conventional Bridgman technique without any purposely added doping agent. High-resistivity InSe single crystals have been obtained by introducing phosphorus in the nonstoichiometric melt $\text{In}_{1.05}\text{Se}_{0.95}$, whose related acceptors compensate the native donor levels.^{15,16} Samples were prepared by cleaving the ingots parallel to the layers (perpendicular to the c axis). For capacitance measurements the samples were cut into slabs 5–30 μm thick and $4 \times 4 \text{ mm}^2$ in size. The thickness of the slabs was measured by means of the interference fringe pattern in the near-infrared region. Gold electrodes were vacuum evaporated in the large sample faces. Ohmic contacts were made by soldering silver leads to the electrodes with high-purity indium. The capacitance of the samples was measured by using a high-accuracy capacitance meter and shielded leads.

Hydrostatic pressure measurements were carried out up to 1.2 GPa by using a piston-cylinder Unipress copper-

beryllium cell with a 4:1 methanol-ethanol mixture as pressure transmitting fluid. In addition, measurements under quasi-hydrostatic conditions up to 3 GPa were carried out using a Bridgman cell which has been described in Ref. 13. In the present case, we have used tungsten carbide anvils 27 mm in diameter. Gaskets were made of pyrophyllite pre-treated at 720 °C during one hour in order to get suitable mechanical properties,¹⁷ and the pressure-transmitting medium was sodium chloride. The pressure was determined by calibration of the oil pressure of the 150-ton press used against known fixed points.¹⁸ Temperature measurements of the capacitance were performed in a helium closed cycle Leybold Hereaus cryogenic system.

Afterwards, to determine the temperature dependence of both the ordinary (n_{\perp}) and the extraordinary (n_{\parallel}) refractive indexes, the samples were heated in a system implemented at the laboratory. For these measurements, the thickness of the used samples was between 10 and 30 μm . The thickness was obtained from the interference fringe pattern in a large spectral range by assuming the curves of n_{\perp} as a function of wavelength (λ) given by Refs. 19 and 20. The ordinary refractive index as a function of temperature was measured from the shift of the interference fringe pattern in the near infrared ($\lambda \geq 1000$ nm) transmission spectra at normal incidence. The extraordinary refractive index was determined from transmission spectra at oblique incidence with polarization parallel to the plane of incidence. Under these conditions, fringe minima are given by²¹

$$m = \frac{2n_{\perp}d}{\lambda} \left(1 - \frac{\sin^2 \theta}{n_{\parallel}^2} \right), \quad (1)$$

where θ is the incidence angle and m is the interference order, which is identified at RT and normal incidence and can be easily followed in a temperature run. Note that in order to determine n_{\parallel} from Eq. (1), it is necessary to know n_{\perp} for which we have used the results previously established. Finally, fringe pattern spectra were taken at several angles of incidence, and $n_{\parallel}(\lambda)$ curves were obtained for each run; these curves were averaged in order to give the final one.

III. RESULTS

The capacitance (C) at a given pressure and temperature is given by

$$C(P, T) = \epsilon_{\parallel}(P, T) \frac{A(P, T)}{d(P, T)}, \quad (2)$$

where A is the area of the gold electrodes and d is the slab thickness. Then, by means of Eq. (2), we have determined the value of ϵ_{\parallel} , at ambient conditions, from the capacitance measurements in ten to twelve samples with different thickness. In Fig. 1, we have plotted C/A as a function of $1/d$. The linear behavior obtained indicates that our results are not affected by the activation of native shallow impurities. In addition, by performing measurements with the sample embedded and not embedded in the pressure medium, we have verified that the presence of this medium does not produce substantial changes in the capacitance of our samples.²² The value of ϵ_{\parallel} obtained for GaS, GaSe, and InSe is shown

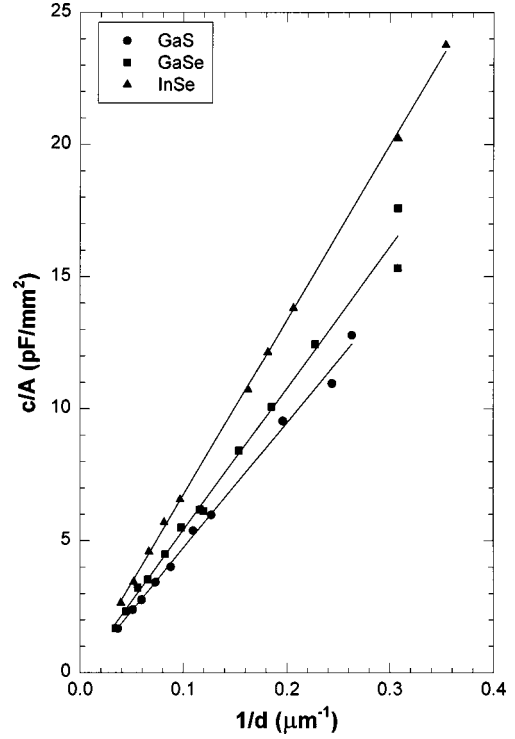


FIG. 1. C/A vs $1/d$ for GaS, GaSe, and InSe.

in Table I. In all cases, it lies in the wide range of values that can be found in the literature,^{14,20,21,23–31} as measured through several techniques, specially infrared reflectivity.

A. Pressure dependence of ϵ_{\parallel}

We first examine the effects of pressure on ϵ_{\parallel} . To obtain $\epsilon_{\parallel}(P)$ from $C(P)$ we have used Eq. (2). One must take into account the pressure changes in the sample dimensions through the parallel (χ_{\parallel}) and perpendicular (χ_{\perp}) compressibilities.^{10–12} Figure 2 shows the pressure dependence of the parallel low-frequency dielectric constant obtained under hydrostatic conditions for three different samples of GaSe. In this figure, it can be seen that ϵ_{\parallel} has a similar behavior to that observed previously in GaS.¹⁴ Figure 3 gives ϵ_{\parallel} as a function of pressure up to 3 GPa for GaS, GaSe, and InSe. Notice that, in the range of pressure up to 1.2 GPa, these results confirm those obtained under hydrostatic conditions (see Fig. 2 and Ref. 14). In addition, from Fig. 3, one can observe that, in the three layered compounds studied here, the pressure coefficient $\partial(\ln \epsilon_{\parallel})/\partial P$ is positive within the whole range of pressures, quite in contrast with the case of tetrahedrally coordinated semiconductors. The values of this coefficient at $P=0$ and 3 GPa are listed in Table II.

TABLE I. Value of ϵ_{\parallel} at ambient conditions for GaS, GaSe, and InSe as obtained from capacitance measurements.

| Material | ϵ_{\parallel} | | References |
|----------|------------------------|------------|---------------|
| | Present work | Literature | |
| GaS | 5.3 ± 0.3 | 5.2–6.6 | 14, 29–31 |
| GaSe | 6.1 ± 0.3 | 6.1–7.9 | 27, 28 |
| InSe | 7.6 ± 0.4 | 6.8–8.5 | 20, 21, 23–26 |

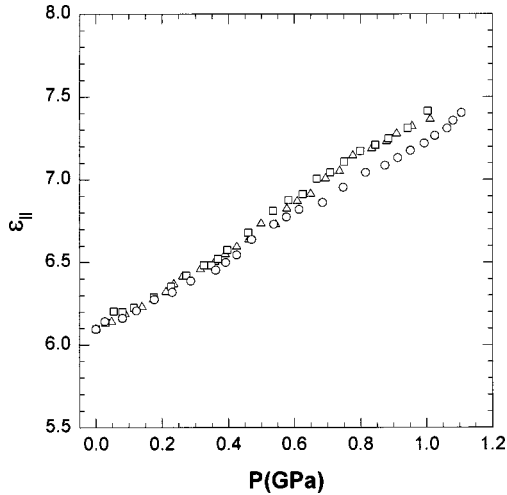


FIG. 2. Piston-cylinder measurements of the low-frequency dielectric constant parallel to c axis for three different samples of GaSe.

In Fig. 3, it can be also seen that in GaSe, the behavior of $\varepsilon_{||}$ is nearly linear up to around 1.8 GPa; above this pressure a reduction of the slope takes place. These results are just between those expected from the isotrope and the charge transfer hypothesis proposed by Gauthier *et al.*¹⁰ For InSe the same kind of pressure dependence has been observed but the change in the slope occurs at around 1 GPa. This is coherent with the higher ionicity of InSe, which can be viewed as inducing an inner pressure via Coulomb interactions³² making the InSe analogous to the pressurized GaSe.

Regarding GaS, between 1.5 GPa and 1.8 GPa, an abrupt increase in $\varepsilon_{||}$ has been observed. However, above 1.8 GPa its pressure dependence is almost the same as that observed below 1.5 GPa. It is important to notice that upon decompression, the strong change of $\varepsilon_{||}$ observed between 1.5 GPa

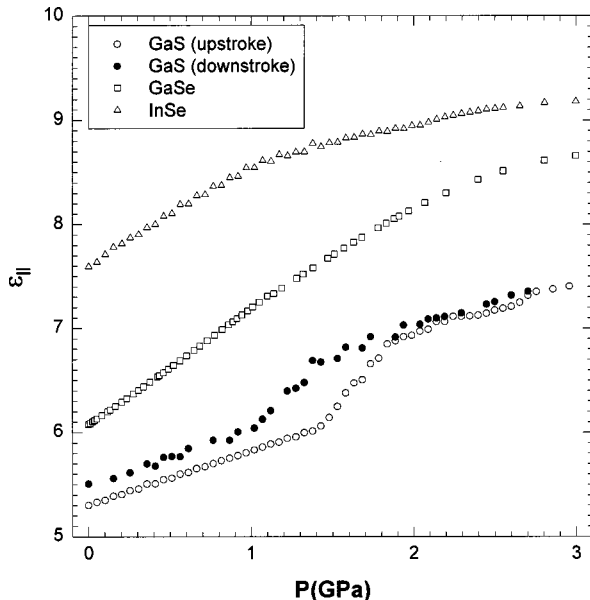


FIG. 3. Pressure dependence of the low-frequency dielectric constant parallel to c axis as obtained from capacitance measurements in a Bridgman cell.

TABLE II. Values of the logarithmic pressure and temperature derivatives of $\varepsilon_{||}$ as deduced from the present results.

| Material | $\partial(\ln \varepsilon_{ })/\partial P$ [10^{-3} GPa^{-1}] | $\partial(\ln \varepsilon_{ })/\partial P$ [10^{-3} GPa^{-1}] | $\partial(\ln \varepsilon_{ })/\partial T$ [10^{-5} K^{-1}] | $\partial(\ln \varepsilon_{ })/\partial T$ [10^{-5} K^{-1}] |
|----------|---|---|---|---|
| | $P = 1 \text{ atm}$ | $P = 3 \text{ GPa}$ | $T = 300 \text{ K}$ | $T = 40 \text{ K}$ |
| GaS | 85 ± 5 | 55 ± 5 | 83 ± 5 | 50 ± 5 |
| GaSe | 135 ± 10 | 57 ± 5 | 74 ± 5 | 45 ± 5 |
| InSe | 120 ± 10 | 32 ± 5 | 72 ± 5 | 36 ± 5 |

and 1.8 GPa seems to be reversible (see Fig. 3), besides a hysteresis of 0.4 GPa. A similar behavior has been obtained previously in the pressure dependence of the ordinary refractive index at around 1.6 GPa.³³ These changes in the optical constants are related with a pressure-induced reversible phase transition that occurs without destruction of single crystals.³⁴ This phase transition leads to a more compact new phase in which an enhancement of the charge density is expected. This enhancement causes the observed increase of $\varepsilon_{||}$. The fact that the change of $\varepsilon_{||}$ is not so abrupt, as the one observed in n_{\perp} ,³³ is due to the presence of uniaxial stress in our measurements which were carried out in a solid medium.

B. Temperature dependence of $\varepsilon_{||}$, n_{\perp} , and $n_{||}$

We next consider the effects of temperature on $\varepsilon_{||}$ and the refractive indexes. To obtain $\varepsilon_{||}(T)$ from $C(T)$ we have used again Eq. (2), but now the correction for the thermal expansion of the samples has been neglected, bearing in mind that it leads to a correction several orders of magnitude lower than the experimental errors. Figure 4 shows the temperature dependence of $\varepsilon_{||}$, that turns out to be nonlinear. In particular, a reduction in the temperature coefficient $\partial(\ln \varepsilon_{||})/\partial T$, as the temperature decreases, has been observed (see Table II).

The $n_{\perp}(\lambda)$ and $n_{||}(\lambda)$ spectra of GaS sample at different temperatures are shown in Fig. 5(a). Similar spectra have been obtained for GaSe and InSe [see Figs. 5(b) and 5(c)], respectively. Figure 6 shows the temperature dependence of the ordinary and extraordinary refractive indexes in the three

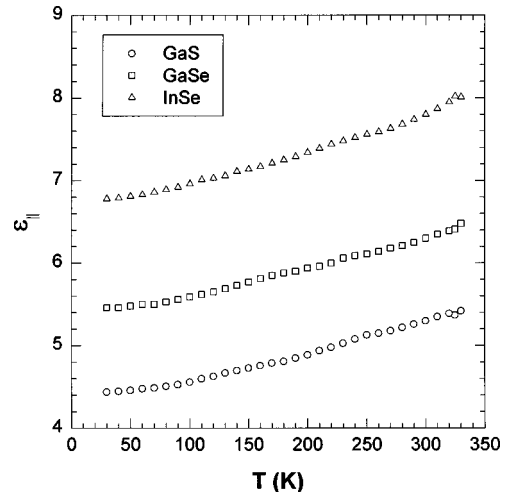


FIG. 4. Temperature dependence of the low-frequency dielectric constant parallel to c axis as obtained from capacitance measurements.

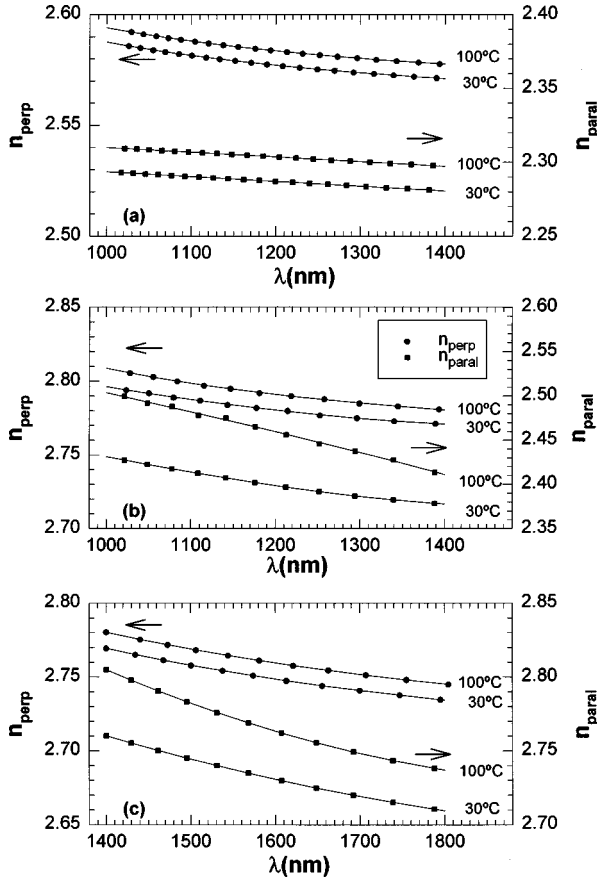


FIG. 5. The refractive indexes of (a) GaS, (b) GaSe, and (c) InSe at 30°C and 100°C as obtained from fringe measurements.

compounds studied here. In all of them we have observed an increase of both $n_{\perp}(\lambda)$ and $n_{\parallel}(\lambda)$ with increasing temperature. Their temperature coefficients $\partial(\ln n_{\perp})/\partial T$ are summarized in Table III and agree with the data found in the literature⁵⁻⁷ in the wavelength region where comparison is possible.

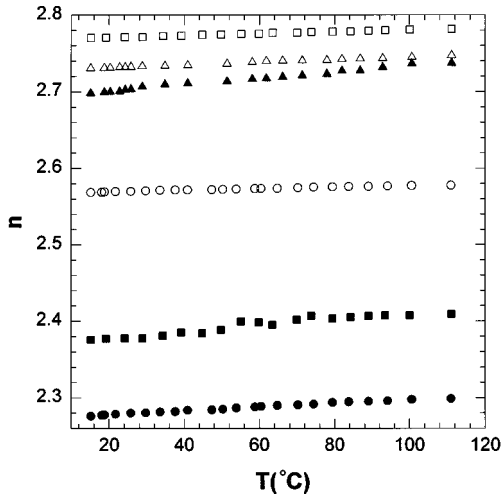


FIG. 6. Temperature dependences of both the ordinary (empty symbols) and the extraordinary (full symbols) refractive index for GaS (○), GaSe (□), and InSe (△).

TABLE III. Temperature coefficient of the ordinary and extraordinary refractive index at $\lambda=1400$ nm (1800 nm for InSe). The temperature coefficient of $\varepsilon_{\infty\parallel}$ and $\varepsilon_{L\parallel}$ are also given.

| Material | $\partial(\ln n_{\perp})/\partial T$ [10^{-5} K^{-1}] | $\partial(\ln n_{\parallel})/\partial T$ [10^{-5} K^{-1}] | $\partial(\ln \varepsilon_{\infty\parallel})/\partial T$ [10^{-5} K^{-1}] | $\partial(\ln \varepsilon_{L\parallel})/\partial T$ [10^{-5} K^{-1}] |
|----------|--|--|--|---|
| GaS | 3.5 ± 0.3 | 10.1 ± 0.5 | 20 ± 1 | 620 ± 80 |
| GaSe | 4.3 ± 0.3 | 13.8 ± 0.5 | 17 ± 1 | 850 ± 110 |
| InSe | 5.8 ± 0.5 | 14.5 ± 0.5 | 18 ± 1 | 600 ± 70 |

IV. DISCUSSION

Before entering into the discussion of the present experimental results, we will briefly bring forward some theoretical considerations. The low-frequency dielectric constant of a heteropolar semiconductor can be written as

$$\varepsilon = \varepsilon_{\infty} + \varepsilon_L, \quad (3)$$

where $\varepsilon_{\infty} = n^2$ is the electronic contribution to the dielectric constant and ε_L is the lattice contribution, which arises because the longitudinal-optical (LO) mode produces a macroscopic electric moment in these semiconductors. These contributions are given by³⁵

$$\varepsilon_{\infty} = 1 + \frac{E_P^2}{E_0^2}, \quad (4)$$

where E_P is the plasma energy of valence electrons, and E_0 is the Penn gap, and

$$\varepsilon_L = \frac{Ne_T^{*2}}{\varepsilon_0 M \omega_{TO}^2}, \quad (5)$$

where ε_0 is the vacuum permittivity, N is the number of unit cells per unit volume, e_T^* is the transverse dynamic effective charge, M is the reduced mass of the polar mode, and ω_{TO} is the frequency of the transverse-optical (TO) mode. Notice that a simple one-gap model³⁶ has been assumed for ε_{∞} . From Eq. (3) it can be shown that

$$\left[\frac{\partial \ln \varepsilon}{\partial P} \right]_T = \frac{\varepsilon_{\infty}}{\varepsilon} \left[\frac{\partial \ln \varepsilon_{\infty}}{\partial P} \right]_T + \frac{\varepsilon_L}{\varepsilon} \left[\frac{\partial \ln \varepsilon_L}{\partial P} \right]_T \quad (6)$$

and a similar expression can be deduced for the temperature derivatives. In the case of III-VI semiconductors Eqs. (3)–(6) must be written for both polarizations, perpendicular and parallel to c axis. The electronic and lattice contributions to ε_{\parallel} have been measured by several authors.^{10,23,29} Unfortunately, the reported values of $\varepsilon_{\infty\parallel}$ and $\varepsilon_{L\parallel}$ exhibit a large dispersion, which explains the large errors attributed to them in Table IV. In spite of the dispersion, all results agree in the small value of the lattice contribution to ε_{\parallel} .

A. Electronic and lattice contributions to ε_{\parallel} and their pressure dependences

In order to explain the large increase of ε_{\parallel} , the charge transfer model¹⁰ focuses on the lattice contribution and proposes an increase of the effective charge $e_{T\parallel}^*$ due to a charge transfer from the cation-cation bond to the interlayer space. That mechanism is suggested by the pressure behavior of the

TABLE IV. Values of the optical and lattice contributions to ε_{\parallel} at ambient conditions. Last column shows the photoelastic parameter.

| Material | $\varepsilon_{\infty\parallel}$ | $\varepsilon_{L\parallel}$ | κ'_{\parallel} |
|----------|---------------------------------|----------------------------|-----------------------|
| GaS | 5.1 ± 0.2 | 0.55 ± 0.05 | 3.0 ± 0.3 |
| GaSe | 5.7 ± 0.2 | 0.42 ± 0.05 | 6.5 ± 0.7 |
| InSe | 7.0 ± 0.3 | 0.70 ± 0.10 | 4.0 ± 0.4 |

phonon modes whose frequency critically depends on the force constant associated with the cation-cation bond. In Raman experiments under pressure, a frequency decrease (or very weak increase) of those modes is actually observed,¹⁰ indicating a weakening of the cation-cation bond.

Nevertheless, the existence of such charge transfer does not necessarily lead to an increase of the dynamic charge for polarization parallel to the c axis. From the point of view of the band structure, this charge transfer could be seen as an increase of the weight of the In s antibonding or the Se p_z nonbonding states in the valence bands. In a rigid ion scheme, the first possibility would have little effect on the overall charge associated with them, as one would expect the electron density associated with In related states to follow the In atoms movement (that vibrate in phase in the LO polar mode). The second possibility would result in an increase of the electron density around the anions and, consequently, in an increase of both $e_{T\parallel}^*$ and $e_{T\perp}^*$. This is hardly compatible with the observed decrease of the effective charge perpendicular to the c axis $e_{T\perp}^*$.¹⁰ Quantitative predictions of the charge transfer hypothesis¹⁰ are based on the assumption that the total dynamic charge remains constant under pressure. However, an increase of the crystal ionicity under pressure could result in an overall change of the dynamical effective charge, as there is no physical principle stating the constancy of this quantity that, in fact, has been shown to decrease under pressure in III-V semiconductors.¹

On the other hand, according to the isotropy scheme,¹⁰ ε_{\parallel} must suffer a drastic evolution since III-VI semiconductors around 5 GPa should behave macroscopically as isotropic materials. However, within this assumption, ε_{\parallel} should be about 10.5 at 5 GPa in GaSe, whereas an extrapolation of our results would give a value not higher than 9 for ε_{\parallel} at that pressure. In addition, examination of Fig. 3 reveals that the increase observed in InSe is smaller than the one expected according to this scheme.⁹ In fact, the isotropy scheme is a mere phenomenological hypothesis that can hardly result in a model accounting for the pressure dependence of basic physical quantities.

We will now discuss a possible explanation of the experimentally observed behavior of ε_{\parallel} under pressure, trying at

the same time to elucidate the origin of it. In order to do so, we choose a rigid ion scheme. According to this model, if we call ϕ the angle between the anion-cation bond and the layer plane, the relationship between the transverse effective charges could be roughly estimated as $e_{T\parallel}^*/e_{T\perp}^* = tg \phi$. In the case of InSe, for which $\phi = 28.4^\circ$, it yields $e_{T\parallel}^*/e_{T\perp}^* = 0.53$, in good agreement with its actual value, 0.47 ± 0.05 .¹⁰ It has been shown recently that the angle ϕ increases under pressure in GaSe and InSe (Ref. 37) at a rate of 5.1×10^{-3} rad/GPa, and in GaTe (Ref. 38) at a rate of 4×10^{-3} rad/GPa. From previous Raman scattering results, it was determined that the effective charge $e_{T\perp}^*$ in GaSe decreases under pressure, at a rate of $\partial(\ln e_{T\perp}^*)/\partial P = -8.7 \times 10^{-3}$ GPa⁻¹.¹⁰ A similar behavior for $e_{T\perp}^*$ can be deduced in InSe, where $\partial(\ln e_{T\perp}^*)/\partial P = -11.2 \times 10^{-3}$ GPa⁻¹.³⁸ Then, one can easily calculate that, within the framework of the rigid ion model, the pressure increase of $e_{T\parallel}^*$ is given by

$$\frac{\partial \ln e_{T\parallel}^*}{\partial P} = \frac{\partial \ln e_{T\perp}^*}{\partial P} + \frac{\partial \phi}{\partial P} \sin \phi \cos \phi. \quad (7)$$

The values obtained for $\partial(\ln e_{T\parallel}^*)/\partial P$ by applying this equation are shown in Table V. In addition, from Eq. (5), it is straightforward to derive the pressure coefficient of $\varepsilon_{L\parallel}$:

$$\frac{\partial \ln \varepsilon_{L\parallel}}{\partial P} = \chi + 2 \frac{\partial \ln e_{T\parallel}^*}{\partial P} - 2 \frac{\partial \ln \omega_{TO\parallel}}{\partial P}, \quad (8)$$

where $\chi = 2\chi_{\perp} + \chi_{\parallel}$ is the volume compressibility, which is well known in the layered materials here studied.¹⁰⁻¹² The pressure coefficient $\partial(\ln \omega_{TO\parallel})/\partial P$ in layered semiconductors has not been measured yet, but this coefficient spans in a range of $(15-20) \times 10^{-3}$ GPa⁻¹ for A1 nonpolar modes in InSe (Ref. 39) and GaSe.¹⁰ Therefore, in Eq. (8), the shift towards higher energies of the TO mode under compression^{10,38} compensates the positive contribution of the first two terms. Then, by assuming for χ and $\partial(\ln \omega_{TO\parallel})/\partial P$ the values shown in Table V, Eq. (8) yields $\partial(\ln \varepsilon_{L\parallel})/\partial P$ of the order of 8×10^{-3} GPa⁻¹ for InSe and of -2×10^{-3} GPa⁻¹ for GaSe. With Eq. (6) and the data from Table IV the contribution of $\varepsilon_{L\parallel}$ to the increase of ε_{\parallel} under pressure turns out to be in absolute value $|(\varepsilon_{L\parallel}/\varepsilon_{\parallel})\partial(\ln \varepsilon_{L\parallel})/\partial P| \leq 10^{-3}$ GPa⁻¹ and can be safely neglected. It follows that the main contribution to the increase of ε_{\parallel} under pressure must come from the electronic contribution $\varepsilon_{\infty\parallel}$. This conclusion is in agreement with the behavior of the extraordinary refractive index n_{\parallel} in GaS that exhibits a strong increase under pressure.^{17,21} The pressure coefficient of $\varepsilon_{\infty\parallel}$ in GaS, as deduced from the refractive index increase,

TABLE V. Pressure coefficient of the perpendicular and parallel effective charges, the parallel TO phonon mode, and $\varepsilon_{L\parallel}$. The compressibility and $\partial\phi/\partial P$ are also given.

| Material | $\partial(\ln e_{T\perp}^*)/\partial P$ [10^{-3} GPa ⁻¹] | $\partial\phi/\partial P$ [10^{-3} rad/GPa] | $\partial(\ln e_{T\parallel}^*)/\partial P$ [10^{-3} GPa ⁻¹] | χ [10^{-3} GPa ⁻¹] | $\partial(\ln \omega_{TO\parallel})/\partial P$ [10^{-3} GPa ⁻¹] | $\partial(\ln \varepsilon_{L\parallel})/\partial P$ [10^{-3} GPa ⁻¹] |
|----------|--|---|--|---|--|--|
| GaSe | -8.7 | 5.1 | 3.4 | 35 | 17 ± 3 | 8 ± 6 |
| InSe | -11.2 | 5.1 | 0.9 | 30 ± 3 | 17 ± 3 | -2 ± 6 |

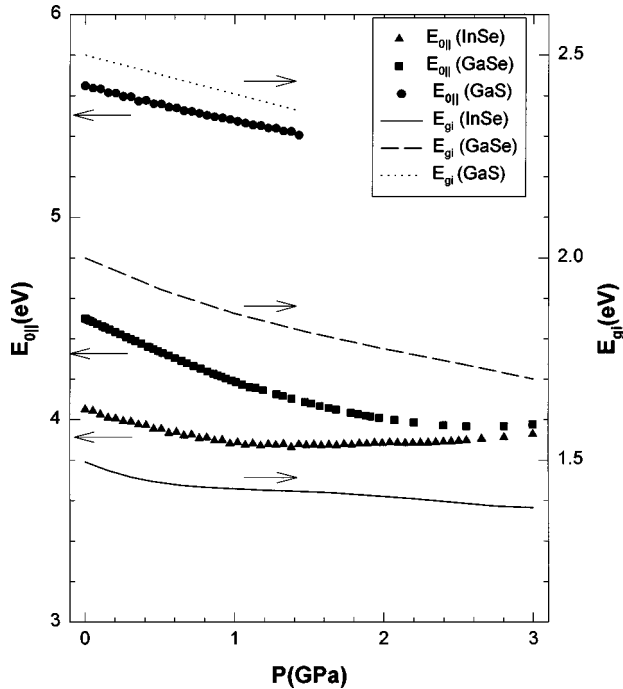


FIG. 7. Pressure dependence of $E_{0||}$ for GaS, GaSe, and InSe as obtained from our experimental results. The lines represent the pressure dependence of the indirect band gap.

is $(90 \pm 10) \times 10^{-3} \text{ GPa}^{-1}$. This value is, within errors, very close to that of $\varepsilon_{||}$, as obtained from capacitance measurements (Table II).

In this context, it is of interest to discuss this result in relation with the Weintstein *et al.*⁴⁰ criterion of bond dimensionality. If we assume that the increase of $\varepsilon_{||}$ is mainly of electronic origin, the photoelastic parameter $\kappa'_{||} = -\partial \ln(\varepsilon_{\infty||} - 1) / \partial \ln V$ can be estimated from the pressure coefficient of $\varepsilon_{||}$. The result is shown in the last column of Table IV. There it can be seen that $\kappa'_{||}$ turns out to be large and positive, suggesting that, along the c axis, III-VI layered semiconductors behave as molecular solids, i.e., their optical properties for polarization parallel to the c axis would be dominated by the band widening produced by the increase of interlayer interactions.

From another point of view, the strong increase of $\varepsilon_{\infty||}$ under pressure in these materials can be correlated to the increase of this quantity in the series GaS-GaSe-InSe (Table IV) through their band structure. According to recent LMTO calculations in InSe,⁴¹ near to the border of the first Brillouin zone, the upper valence band (with anion p_z character) runs parallel to the lowest conduction band (with cation p_y character), which yields a high joint density of states. The transition is fully allowed for polarization parallel to the c axis. Let us assume, in the framework of a simplified one-gap Phillips-van Vechten model, that this transition corresponds to the effective Penn gap $E_{0||}$ determining $\varepsilon_{\infty||}$ through Eq. (4). If we calculate the plasma energy from the valence band electron density, $E_{0||}$ can be obtained from $\varepsilon_{\infty||}$. The result is shown in Table V. This table also shows, for the sake of comparison, the value of the indirect gap E_{gi} and its pressure coefficient for each compound.^{10,42,43} In this model, these transitions must be correlated, as they share the same final state (the conduction band minimum at the zone border). The

TABLE VI. Van Vechten model parameters and indirect band gap for GaS, GaSe, and InSe. The pressure coefficient of the Penn gap and of the indirect band gap are also given.

| Material | $E_{0 }$ [eV] | $E_{P }$ [eV] | $\partial E_{0 } / \partial P$ [meV/GPa] | E_{gi} [eV] | $\partial E_{gi} / \partial P$ [meV/GPa] |
|----------|-----------------|----------------|---|---------------|--|
| GaS | 5.50 ± 0.15 | 11.44 | -200 ± 10 | 2.5 | -110 ± 10 |
| GaSe | 4.76 ± 0.15 | 10.77 | -360 ± 30 | 2.0 | -150 ± 20 |
| InSe | 3.85 ± 0.15 | 9.90 | -210 ± 20 | 1.6 | -60 ± 10 |

pressure dependence of the Penn gap can be calculated, from our results, by means of Eq. (4), taking into account the compressibility of each compound, that enters in the pressure dependence of $E_{P||}$. The results are shown in Fig. 7 and the pressure coefficient at room pressure can be seen in Table VI. The results illustrated in Fig. 7 show that the pressure dependence obtained for $E_{0||}$ is very similar to that of E_{gi} . This, together with the fact that both the energy and pressure coefficient of $E_{0||}$ and E_{gi} scale in the three compounds, appears as an indication of the plausibility of the present model and supports the electronic origin of the large pressure increase of $\varepsilon_{||}$.

B. Temperature dependences

First, we want to point out some remarks regarding the temperature dependence of $n_{||}$. The temperature derivative $\partial n_{||} / \partial T$ can be calculated at different wavelengths by assuming that $n_{||}$ varies linearly with T in the range between 0°C and 120°C . It can be seen from Fig. 5(a) that in GaS, this derivative seems to be nearly constant between $\lambda = 1000 \text{ nm}$ and $\lambda = 1400 \text{ nm}$. Instead of that, in GaSe $\partial n_{||} / \partial T$ depends on the wavelength [see Fig. 5(b)]. The resulting dependence of this derivative is shown in Fig. 8 (solid line); a similar behavior is obtained for InSe. We think that this difference is related to the proximity of the absorption edge of GaSe and InSe to the region where the measurements were carried out. In fact, in InSe the wavelength had to be extended beyond 1400 nm since the presence of a

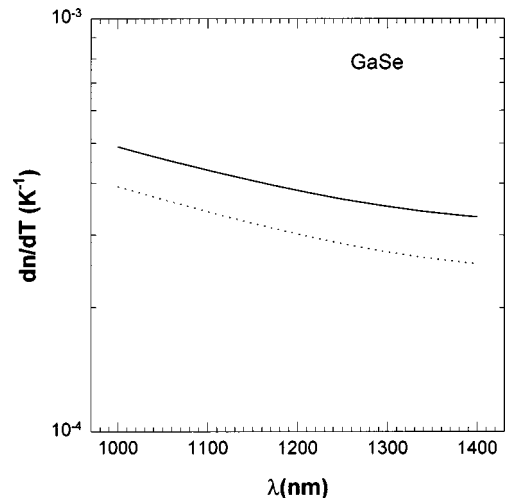


FIG. 8. Temperature coefficient of the extraordinary refractive index of GaSe as a function of photon wavelength (solid line). The dotted line represents the effective coefficient.

TABLE VII. Volume thermal expansion coefficient, compressibility, and $\partial(\ln E_{0\parallel})/\partial T$ for GaS, GaSe, and InSe. The logarithmic temperature derivative of the smallest band gap (E_g) is also given for comparison.

| Material | β [10^{-6} K^{-1}] | χ [10^{-3} GPa^{-1}] | $\partial(\ln E_{0\parallel})/\partial T$ [10^{-4} K^{-1}] | $\partial(\ln E_g)/\partial T$ [10^{-4} K^{-1}] |
|----------|---|--|---|--|
| GaS | 27.5 | 33 | -1.67 | -2 |
| GaSe | 30.5 | 35 | -1.85 | -2.38 |
| InSe | 44.5 | 30 \pm 3 | -2.08 | -2.62 |

strong peak at $\lambda \approx 990 \text{ nm}$ affects the temperature coefficient of n_{\parallel} . Finally, we note that the decrease of $\partial n_{\parallel}/\partial T$ with increasing λ (see Fig. 8) obtained from our data is not in complete agreement with the previously reported results for GaSe.^{6,27} This disagreement can be related to the fact that those measurements were carried out in a range of energies including the exciton absorption line. Considering this, the effects of the shift of the direct band gap (E_{gd}) in $\partial n_{\parallel}/\partial T$ must be taken into account in order to calculate $\partial(\ln \varepsilon_{\infty\parallel})/\partial T$ in GaSe and InSe.

Let us assume, as a first approximation, that the absorption edge is given by a step function. In that case, it can be easily shown that

$$\frac{\partial(\Delta n_{\parallel})}{\partial T} = \frac{-2\hbar c \alpha_0}{\pi} \frac{(\partial E_{gd}/\partial T)}{E_{gd}^2 - E^2}, \quad (9)$$

where $\partial(\Delta n_{\parallel})/\partial T$ is the variation of n_{\parallel} due to the shift of the direct band gap with the temperature, α_0 is the absorption coefficient and E is the photon energy. Thus, using for GaSe, $\alpha_0 = 4 \times 10^4 \text{ cm}^{-1}$,⁴⁴ $E_{gd} = 2.0196 \text{ eV}$,¹⁰ and $\partial E_{gd}/\partial T = -0.5 \text{ meV/K}$,⁴⁵ one can evaluate the effective temperature derivative $\partial n_{\parallel}^*/\partial T$ from which we have calculated $\partial(\ln \varepsilon_{\infty\parallel})/\partial T$. The dotted line of Fig. 8 shows $\partial n_{\parallel}^*/\partial T$ as a function of λ . We have also calculated $\partial(\ln \varepsilon_{\infty\parallel})/\partial T$ for InSe with the same approximation. The obtained values for this coefficient in the three compounds are shown in Table III.

The temperature dependence of $\varepsilon_{\infty\parallel}$ can be understood with the help of Eq. (4). From this equation it can be deduced that the temperature coefficient of the electronic dielectric constant is given by

$$\frac{\partial \ln(\varepsilon_{\infty\parallel} - 1)}{\partial T} = -\beta + \frac{2\beta}{\chi} \frac{\partial \ln E_{0\parallel}}{\partial P} - 2 \frac{\partial \ln E_{0\parallel}}{\partial T}, \quad (10)$$

where β is the volume thermal expansion coefficient. Then, by taking χ and β from the literature^{10-12,31,46,47} and using the values previously deduced for $\partial E_{0\parallel}/\partial P$, it can be seen that the two first terms of Eq. (10), which account for the effect of thermal expansion, are always negative. Would this be the only operative mechanism, it would lead to a negative value of $\partial(\ln \varepsilon_{\infty\parallel})/\partial T$. Then, in order to account for the experimental temperature behavior of $\varepsilon_{\infty\parallel}$, a decrease of the Penn gap with increasing temperature must be assumed. The obtained values for $\partial(\ln E_{0\parallel})/\partial T$ are summarized in Table VII. In this table, the logarithmic temperature derivative of the fundamental gap is also given for comparison and turns out to be very close to that of the Penn gap in each semiconductor.^{45,48,49} The temperature dependence of the

fundamental gap in III-VI semiconductors is known to be determined by the interaction of electrons with homopolar optical phonons.^{50,51} In function of the results shown in Table VII and taking into account that the self-energy contribution to the fundamental gap arises mainly from the valence band,⁵¹ it is reasonable to assume that the temperature dependence of the Penn gap is also determined by electron-phonon interaction.

On the other hand, as the experimental value of $\partial(\ln \varepsilon_{\infty\parallel})/\partial T$ is at least four times smaller than the temperature coefficient of ε_{\parallel} (see Tables II and III), the temperature increase of ε_{\parallel} cannot be explained only with the increase of $\varepsilon_{\infty\parallel}$. Then, from these results and by means of an expression analogous to Eq. (6), we have estimated the temperature coefficient of the lattice contribution to ε_{\parallel} . The values of this coefficient for GaS, GaSe, and InSe are given in Table III. The logarithmic temperature derivative of $\varepsilon_{L\parallel}$ is considerably larger than the corresponding derivative of $\varepsilon_{\infty\parallel}$. By comparison with II-VI and III-V compounds, $\varepsilon_{\infty\parallel}$ exhibits a normal response, but the temperature coefficient of $\varepsilon_{L\parallel}$ is one order of magnitude larger than the one observed in tetrahedrally coordinated semiconductors.¹ From Eq. (5), it is straightforward to deduce

$$\begin{aligned} \frac{\partial \ln \varepsilon_{L\parallel}}{\partial T} = & -\beta - \frac{2\beta}{\chi} \frac{\partial \ln e_{T\parallel}^*}{\partial P} + 2 \frac{\partial \ln e_{T\parallel}^*}{\partial T} + \frac{2\beta}{\chi} \frac{\partial \ln \omega_{\text{TO}\parallel}}{\partial P} \\ & - 2 \frac{\partial \ln \omega_{\text{TO}\parallel}}{\partial T}. \end{aligned} \quad (11)$$

From the data given in Tables V and VII, the first, second, and third term give neglectable contributions. As regards the last term, as the temperature coefficients of phonon modes are very small (of the order of $-2 \times 10^{-4} \text{ K}^{-1}$),⁵² its contribution is of the order of $4 \times 10^{-4} \text{ K}^{-1}$. Then, in order to account for the large temperature coefficient of $\varepsilon_{L\parallel}$ one must assume a large increase of $e_{T\parallel}^*$ with temperature. This term is related to phonon-phonon interactions (as a consequence of the crystal potential anharmonicity) through the increase of the ion vibration amplitude. Unfortunately, in spite of being topics of constant interest, the effects of these anharmonicities on the effective charge are not well understood. In the case of the layered III-VI semiconductors, we can point out that the polar LO phonon mode (polarized along the c axis) breaks the symmetry of one half layer with respect to the other, which could contribute to an extra mechanism of polarization in which some electronic charge would be transferred between half layers when the vibration amplitude is very large. We stress that this would be an extra mechanism of polarization, that would not appear in a rigid ion scheme. In that case there would be electric polarization without charge transfer between the half layers, as the LO phonon mode changes the angle of the anion-cation bond with respect to the c axis in a opposite way in each half layer. For the sake of completeness we should also point out that this extra mechanism would not contribute to an increase of $e_{T\parallel}^*$ under pressure, as it depends on the vibration amplitude that decreases under pressure (as the phonon frequency increases).

V. CONCLUSIONS

The pressure dependence of ε_{\parallel} of GaS, GaSe, and InSe has been measured up to 3 GPa. We have also measured the temperature dependence of ε_{\parallel} , n_{\parallel} , and n_{\perp} . All these data, combined with earlier results, have led to evaluate the lattice and electronic contributions to the pressure behavior of ε_{\parallel} , that is proposed to be controlled by the large increase of the electronic contribution. This fact was explained through a decrease of the Penn gap, which scales with the decrease of the indirect band gap of III-VI semiconductors. Finally, the temperature behavior of ε_{\parallel} has been discussed. The thermal expansion effects on both the lattice and electronic contribu-

tion have been shown to be neglectable. The electronic contribution is dominated by the temperature decrease of the Penn gap due to electron-phonon interaction. In addition, the strong increase of the lattice contribution with temperature was attributed to an extra mechanism related to the asymmetry between half layers induced by the LO polar mode at large vibration amplitudes.

ACKNOWLEDGMENTS

This work was supported by the Spanish Government CICYT under Grant No. MAT95-0391 and by Generalitat Valenciana under Grant Nos. GV-2205/94 and GV-3235/95.

*Author to whom correspondence should be addressed. Present address: Hochdruckgruppe, Max-Planck-Institut für Chemie, Postfach 3060, D-55020 Mainz, Germany. FAX: (49) 6131 305 330. Electronic address: daniel@mpch-mainz.mpg.de

¹G. A. Samara, Phys. Rev. B **27**, 3494 (1983).

²A. Polian, J. M. Besson, M. Grimsditch, and H. Vogt, Phys. Rev. B **25**, 2767 (1982).

³A. Segura, J. M. Besson, A. Chevy, and M. S. Martin, Nuovo Cimento B **38**, 349 (1977).

⁴R. Le Toullec, N. Piccioli, and J. C. Chervin, Phys. Rev. B **22**, 6162 (1980).

⁵H. Neumann, M. Lorenz, W. Hörig, and F. Lévy, Phys. Lett. **99A**, 437 (1983).

⁶G. Antonioli, D. Bianchi, and P. Franzosi, Appl. Opt. **18**, 3847 (1979).

⁷M. Piacentini, E. Doni, R. Girlanda, V. Grasso, and A. Balzarotti, Nuovo Cimento B **54**, 269 (1979).

⁸N. Kuroda, O. Ueno, and N. Nishina, Phys. Rev. B **35**, 3860 (1987).

⁹A. R. Goñi, A. Cantarero, U. Schwarz, K. Syassen, and A. Chevy, Phys. Rev. B **45**, 4221 (1992).

¹⁰M. Gauthier, A. Polian, J. M. Besson, and A. Chevy, Phys. Rev. B **40**, 3837 (1989).

¹¹A. Polian, M. Grimsditch, M. Fisher, and M. Gattulle, J. Phys. (France) Lett. **43**, L405 (1982).

¹²U. Schwarz, A. R. Goñi, K. Syassen, A. Cantarero, and A. Chevy, High Press. Res. **8**, 396 (1991).

¹³D. Errandonea, A. Segura, J. F. Sánchez-Royo, V. Muñoz, P. Grima, A. Chevy, and C. Ulrich, Phys. Rev. B **55**, 16217 (1997).

¹⁴A. Segura and A. Chevy, Phys. Rev. B **49**, 4601 (1994).

¹⁵A. Chevy, J. Cryst. Growth **67**, 119 (1984).

¹⁶A. Chevy, J. Appl. Phys. **56**, 978 (1984).

¹⁷M. Nishikawa and S. Akimoto, High Temp.-High Press. **3**, 161 (1971).

¹⁸H. T. Hall, Rev. Sci. Instrum. **33**, 1278 (1962).

¹⁹T. A. McMath and J. C. Irvin, Phys. Status Solidi A **38**, 731 (1976).

²⁰N. Piccioli, R. Le Toullec, F. Bertrand, and J. C. Chervin, J. Phys. (Paris) **42**, 1129 (1981).

²¹J. D. Wasscher and J. Dieleman, Phys. Lett. **39A**, 279 (1972).

²²Taking into account the border effects and the pressure medium, as a first approximation, the capacitance of the samples is given by $C = \varepsilon_{\parallel}(A/d)[1 + \frac{3}{8}(\varepsilon_M/\varepsilon_{\parallel})(d^2/A)]$, where ε_M is the dielectric constant of the pressure medium. According to this, assuming the less favorable situation, i.e., a 30 μm thick sample of GaS embedded in a medium with a dielectric constant equal to

that of methanol ($\varepsilon_M=33$), one obtains a correction to C quite smaller than the experimental error, in accordance with what we have observed.

²³N. Kuroda and Y. Nishina, Solid State Commun. **34**, 481 (1980).

²⁴L. N. Alieva, G. L. Belenkii, I. I. Reshine, and E. Yu Salaev, Fiz. Tverd. Tela (Leningrad) **17**, 51 (1975) [Sov. Phys. Solid State **17**, 90 (1975)].

²⁵N. Gasalny, B. Yavedov, V. Tagirov, and E. Vinogradov, Phys. Status Solidi B **89**, k42 (1978).

²⁶J. Martínez-Pastor, A. Segura, C. Julien, and A. Chevy, Phys. Rev. B **46**, 4607 (1992).

²⁷R. Le Toullec, N. Piccioli, M. Mejatty, and M. Balkanski, Nuovo Cimento B **38**, 159 (1977).

²⁸P. C. Leung, G. Anderman, W. G. Spitzer, and C. A. Nead, J. Phys. Chem. **27**, 849 (1966).

²⁹A. Polian, M. Kuhn, R. Le Toullec, and R. Fornier, in *Proceedings of the 14th International Conference of Physics of Semiconductors*, edited by B. H. L. Wilson (Institute of Physics and Physical Society, London, 1979), p. 907.

³⁰K. R. Allakhverdiev, S. S. Baveev, E. Yu Salaev, and M. M. Tagiev, Phys. Status Solidi B **96**, 177 (1979).

³¹V. Riede, H. Neumann, H. X. Nguyen, H. Sobota, and F. Lévy, Physica (Utrecht) **100**, 355 (1980).

³²J. Aidun, M. S. T. Bukowinski, and M. Ross, Phys. Rev. B **29**, 2611 (1984).

³³I. Rannou, Thèse de Troisième Cycle, Université de Paris VI, 1986.

³⁴H. d'Amour, W. B. Holzapfel, A. Polian, and A. Chevy, Solid State Commun. **44**, 853 (1982).

³⁵G. Martínez, in *Handbook of Semiconductors*, edited by J. S. Moss and M. Balkanski (North-Holland, Amsterdam, 1980), Vol. 2, p. 181.

³⁶D. Penn, Phys. Rev. **128**, 2093 (1962).

³⁷J. P. Itie, A. Polian, M. Gauthier, and A. San Miguel, Highlights ESRF 96/97, edited by ESRF Information Office (ESRF, Grenoble, 1997), p. 57; J. Pellicer-Polles, A. Segura, V. Muñoz, and A. San Miguel, Phys. Rev. B **60**, 3557 (1999).

³⁸J. Pellicer, A. Segura, A. San Miguel, and V. Muñoz, Phys. Status Solidi B **211**, 385 (1999).

³⁹C. Ulrich, M. A. Mogrinski, A. R. Goñi, A. Cantarero, U. Schwarz, and K. Syassen, in *Proceedings of 7th International Conference on High Pressure Semiconductors Physics*, edited by K. Syassen, R. A. Stradling, and A. R. Goñi, [Phys. Status Solidi B **198**, 121 (1996)].

⁴⁰R. A. Weinstein, R. Zallen, M. L. Slade, and A. de Lozanne, Phys. Rev. B **24**, 4652 (1981).

- ⁴¹C. Ulrich, A. R. Goñi, K. Syassen, O. Jepsen, A. Cantarero, and V. Muñoz, *Proceedings of the Joint XV AIRPAT and XXXII EHPRG International Conference*, edited by W. Trzeciakowski (World Scientific, Singapore, 1996), p. 411.
- ⁴²M. Mejatty, A. Segura, R. Le Toulec, J. M. Besson, A. Chevy, and H. Fair, *J. Phys. Chem. Solids* **39**, 25 (1978).
- ⁴³D. Errandonea, F. J. Manjón, J. Pellicer, A. Segura, and V. Muñoz, *Phys. Status Solidi B* **211**, 33 (1999).
- ⁴⁴M. Andriyashiki, M. Yu Sakhnovskii, V. Timofeev, and S. Yakimova, *Phys. Status Solidi* **28**, 277 (1968).
- ⁴⁵S. Kohn, Y. Petroff, and Y. R. Shan, *Surf. Sci.* **37**, 205 (1972).
- ⁴⁶I. G. Karimov, N. G. Aliev, and M. M. Kurbanov, *Fiz. Tekh. Poluprovodn.* **7**, 1050 (1973) [*Sov. Phys. Semicond.* **7**, 1575 (1974)].
- ⁴⁷V. Riede, H. Neumann, F. Lévy, and H. Sobotta, *Phys. Status Solidi B* **109**, 275 (1982).
- ⁴⁸T. Ikari and Y. Koga, *J. Phys. Soc. Jpn.* **47**, 1017 (1979).
- ⁴⁹Y. Depeursinge, *Helv. Phys. Acta* **50**, 589 (1977).
- ⁵⁰J. Camassel, P. Merle, H. Mathieu, and A. Chevy, *Phys. Rev. B* **17**, 4718 (1978).
- ⁵¹Ph. Schmid and J. P. Voitchovsky, *Phys. Status Solidi B* **65**, 249 (1974).
- ⁵²C. Carlone, S. Jandl, and H. R. Shanks, *Phys. Status Solidi B* **108**, 123 (1981).